

XMCD study of the Ruddlesden-Popper Phase $\text{La}_{1.2}\text{Nd}_{0.2}\text{Sr}_{1.6}\text{Mn}_2\text{O}_7$

F. Weigand,^a E. Goering,^a J. Geissler,^a M. Justen,^a K. Dörr,^b K. Ruck^a and G. Schütz^a

^a*Lehrstuhl für Experimentelle Physik IV, Universität Würzburg, Germany. E-mail: frank_w@physik.uni-wuerzburg.de,*
^b*Institut für Festkörper- und Werkstofforschung, Dresden, Germany*

X-ray Magnetic Circular Dichroism (XMCD) measurements of the Ruddlesden-Popper Phase $\text{La}_{1.2}\text{Nd}_{0.2}\text{Sr}_{1.6}\text{Mn}_2\text{O}_7$ are reported. The Mn K, La and Nd $L_{2,3}$ edges have been measured on a powder sample at two different magnetic fields at low temperature. The analysis of the spectra at $B = 1\text{T}$ indicates a large orbital moment of the Nd $5d$ -states and a significant spin-polarization of the La $5d$ -band. Furthermore at the Mn K-edge a XMCD-signal is observed, showing a polarization of the Mn $4p$ -band. At lower field (0.2T) all XMCD-signals are about two times smaller corresponding to the lower total magnetization. The signal at the Nd L_2 edge vanishes completely at 0.2T.

Keywords: x-ray magnetic circular dichroism; manganese; metamagnetism; CMR.

1. Introduction

Since the first publications about ‘Colossal Magneto Resistance’ (CMR) (Helmolt 1993) (Chahara 1993) in perovskite-like $\text{La}_{1-x}\text{M}_x\text{MnO}_x$ ($M=\text{Sr,Ca,Ba}$) ferromagnetic films, a lot of interest was attracted in magnetism related basic research and spin electronics. The CMR systems show a paramagnetic insulator to ferromagnetic metal transition (PI-MI), which is not quantitatively understood up to now. Different models were used to explain the ferromagnetism in magnetic oxides. One model uses double-exchange between two neighboring Mn-ions via the O-ion (Zener 1951). However the disorientation of Mn-spins and the corresponding decrease of kinetic energy are not sufficient enough to describe the paramagnetic insulating phase in CMR materials (Millis 1995) (Millis 1998). Furthermore dynamic coupling of electronic degrees to lattice degrees of freedom (electron-phonon-coupling) should play an important role (Jahn-Teller effect) (Zhao 1996).

In addition to these nearly cubic systems, homologous systems like $(\text{La,Sr})_{n+1}\text{Mn}_n\text{O}_{3n+1}$ (with $n = 1,2,3$) (Moritomo 1996), called Ruddlesden-Popper Phase (Ruddlesden & Popper 1958), are discussed in the last few years. These systems are naturally layered manganites (Battle 1998) (Mitchell 1999) and combine the properties of three-dimensional perovskites with a more two-dimensional behavior (Perring 1997). Their properties like magnetoresistance or magnetic interactions between the different layers depend significantly on the effective dimensionality with changing n from 1 to ∞ (Mahesh 1996) (Seshadri 1997) (Dörr 1999). Neutron-diffraction measurements indicate that layered perovskite systems could be a natural bulk stack of spin-valve devices (Perring 1998).

Our sample $\text{La}_{1.2}\text{Nd}_{0.2}\text{Sr}_{1.6}\text{Mn}_2\text{O}_7$ is of type $n = 2$. Bilayers of perovskite units $(\text{La,Sr})\text{MnO}_3$ are separated by rock-salt like

$(\text{La,Sr})\text{O}$ interlayers. The sample shows CMR effect connected with ferromagnetic behavior below $T_C = 74\text{K}$. Below $T_N = 38\text{K}$ the alternating ferromagnetic bilayers have an anti-ferromagnetic spin arrangement. In external magnetic fields the system undergoes a metamagnetic transition from anti-ferromagnetic to ferromagnetic state at 20K. This transition is continuous, starting at 0.3T and saturating above 1T (Dörr 2000). XMCD measurements of our powder sample are made at the L_2, L_3 edges of La and Nd and the K edge of Mn at different applied magnetic fields at a temperature of 5K.

2. Experimental Procedures and Data Evaluation

The preparation of the polycrystalline sample is explained elsewhere (Dörr 1999). To get a homogenous sample, we ball-milled the sample several times and spread the powder on a tape.

XMCD spectra were recorded at the A1 beamline at HASYLAB with a Si (111) monochromator in two-crystal mode. The energy resolution ($\Delta E/E$) of the monochromatic system was about $5 \cdot 10^{-3}$. A super-conducting magnet system was used and the applied magnetic fields were 0.2 and 1T. For each energy point the magnetic field was flipped. The intensity of the monochromatic incoming beam (I_0) and the transmitted intensity after the sample ($I_{N,S}$) for different magnetic field directions were measured with ionization chambers. During the measurement the sample temperature was kept at 5K. Several spectra were recorded for every edge in order to get a better signal to noise ratio. The raw data were underground subtracted and then the spectra edge normalized. The difference in absorption measured with magnetic fields, parallel and antiparallel to the incoming beam, is the XMCD signal. All dichroic spectra were normalized to the degree of circular polarization. To extract the white line intensity the normal absorption spectra were averaged and an arctan was subtracted, shown in Fig.1. The XMCD effect is visible (La L_2 at 1T about 1% compared to the edge jump).

3. Discussion

As seen in Fig. 1 strong white lines for the La edges are observed due to the narrow unoccupied $5d$ bands, being the final state of the photoabsorption process. The dichroic signal at the La L_2, L_3 edges shows derivative-like behavior at the position of the white line peak. For an applied field of 1T a negative (positive) peak of 2eV FWHM and an amplitude of $-9.5 \cdot 10^5$ ($3.1 \cdot 10^3$) is observed at about +1eV above the L_2 (L_3) edge. These peaks are surrounded by two smaller neighbor peaks at -3 and +3 eV with positive (negative) amplitude.

To compare μ_C at the La L_2, L_3 edges the energy of the first inflection point of the particular edge is set to zero. Furthermore the dichroic signal μ_C of the L_3 edge is multiplied by the factor -2, in order to account the different photoelectron spin polarization ($\sigma_{L_2} = -0.5$; $\sigma_{L_3} = +0.25$) (Fig.2). This reveals a significant spin polarization of the lanthanum $5d$ band. Comparing to previous measurements on the related compound $\text{La}_{0.7}\text{Sr}_{0.3}\text{MnO}_3$ (Kapusta 1996), a small increase in orbital momentum is directly observable, which is enhanced at higher field. No measurable dichroic signal was detected at the La L_1 edge, so the polarization of the La $6p$ band is negligible.

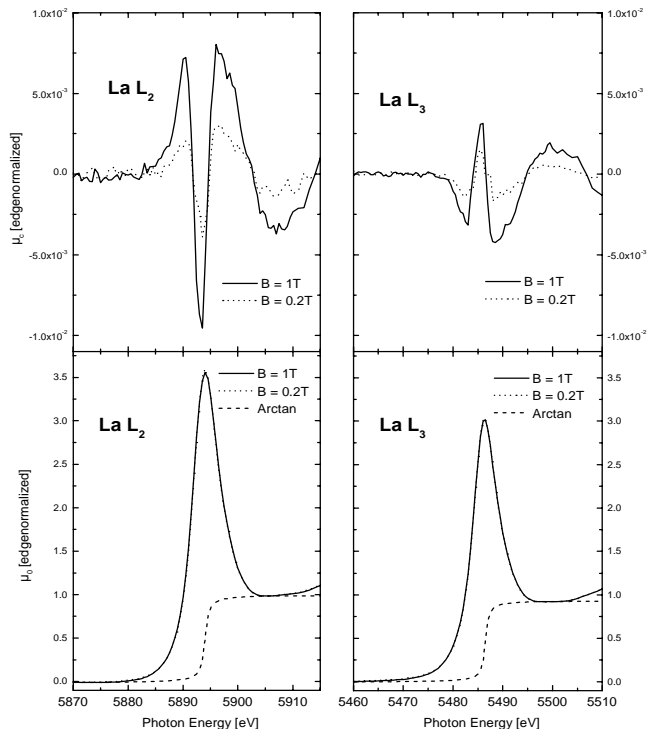


Figure 1
La L₂, L₃, μ_c and μ_0 normalized to the edge step

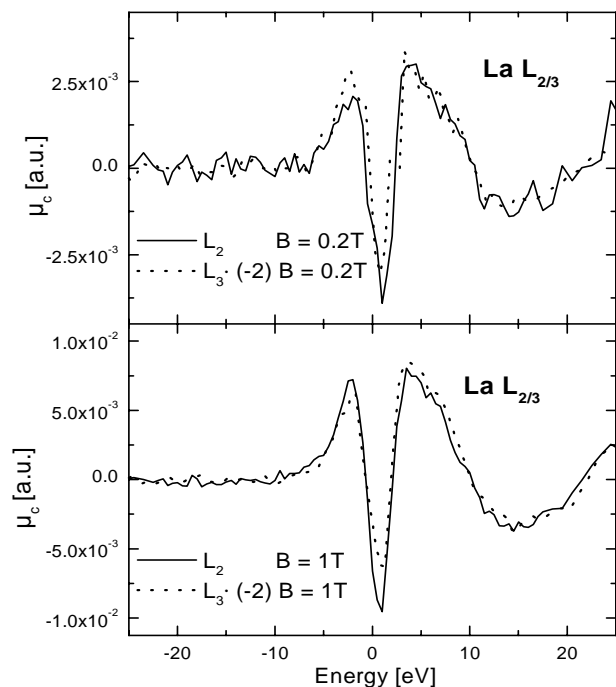


Figure 2
Comparison of μ_c at the La L₂, L₃ edges

The use of sum rules (Thole 1992) (Carra 1993) in the soft X-ray range produces good results for transition metals Fe and Co for the spin and orbital momentum. It is questionable to apply them in hard X-ray range to get quantitative results (Wang 1993) (Jo & Imada 1993) (Galéra et al 1995). Due to the unoccupied 4f shell in La, spin polarized DOS interpretation should be valid

(Baudalet 1993). Unfortunately we do not have SP-DOS calculations up to now for comparing our measurements with theory.

The ratio of the orbital and spin momentum m_{orb}/m_{spin} of the particular band, calculated with sum rules, yields enough information to compare the differences by applying several magnetic fields. The value of m_{orb}/m_{spin} is almost the same for 1T ($4.9 \cdot 10^{-2}$) and 0.2T ($5.4 \cdot 10^{-2}$). At 0.2T these structures are about two times smaller compared to 1T, corresponding to the lower total magnetization observed in SQUID-measurements.

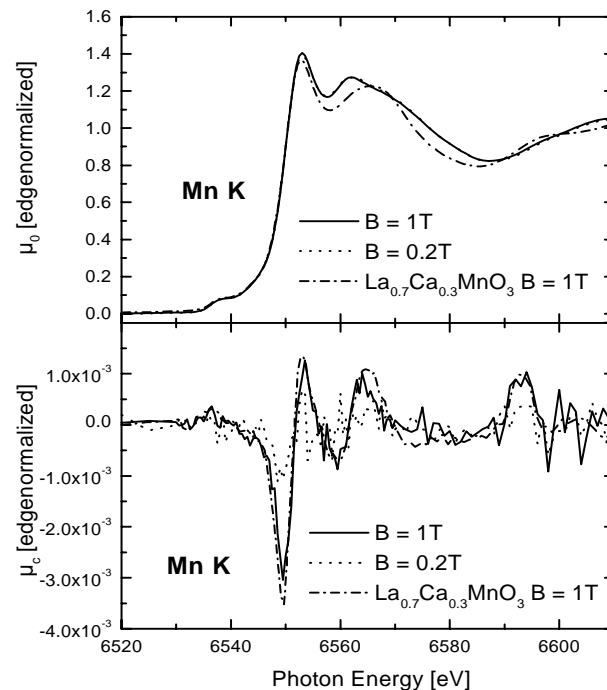


Figure 3
Mn K edge, μ_c and μ_0 normalized to the edge step

At the manganese K edge a weak, negative XMCD signal was detected (Fig.3), showing a small magnetic polarization of the Mn 4p band, corresponding to the polarization of 3d electrons of the parent Mn atom. At 1T it is about two times higher compared to 0.2T. By comparison with equivalent measurements we performed at the La_{0.7}Ca_{0.3}MnO₃ system, a smaller XMCD signal is directly observable. One possibility for this behavior could be a smaller total magnetic moment of the Mn in the Ruddlesden-Popper Phase, caused by non-saturated magnetization. Both systems have nearly the same pre-edge structures in the XANES and XMCD spectra at 6538eV (dipole forbidden transition $1s \rightarrow 3d$), as a result of almost equal averaged valence in the Mn 3d states (Belli 1980). These transition are symmetry allowed due to the mixing of the bounded Mn 3d states with the oxygen 2p band, analogical to related perovskites (García 1995). These structures are comparable to previously published data (Subías 1997).

16eV above the Mn K edge, there is another positive peak in the XMCD signal, which probably originates from magnetic multiple scattering of magnetic nearest-neighbor Mn atoms (Schütz and Ahlers 1997). Another structure is observable at about 43eV above the edge. At this point the energy is high enough to excite 1s and 3p electrons (Subías 1997) simultaneously. These structures are quite the same for La_{1.2}Nd_{0.2}Sr_{1.6}Mn₂O₇ and

$\text{La}_{0.7}\text{Ca}_{0.3}\text{MnO}_3$ showing the different measurements for both systems are comparable and the difference in the XMCD signal at the Mn K edge is real.

The absorption spectra of Nd L_2 , L_3 edges (Fig. 5) show strong white lines. At 1T a very large XMCD signal with an amplitude of $-6 \cdot 10^{-2}$ can be observed at the L_2 edge. The XMCD signal at the L_3 edge is about 10 times smaller. The line shapes of these XMCD signals are comparable to measurements at the Nd L_2 , L_3 edges in the system $\text{Nd}_2\text{Fe}_{14}\text{B}$ (Miguel-Soriano 2000). These structures correspond to strong $5d$ electron polarization, due to the magnetically aligned inner Nd $4f$ shell. Sum rules indicate a projected orbital contribution, which is in the same order (but different sign) as the projected spin contribution. Measurements at the Nd M_4 , M_5 edges show the same behavior for the $4f$ shell (to be published Goering et al.). This could be explained by a non collinear orientation of Nd compared to the total magnetization. Remarkable at lower field of 0.2T is the almost complete vanishing of both dichroic signals. Due to the relative large orbital moment, an applied flipping field of $\pm 0.2\text{T}$ could not be strong enough to change the magnetic direction of the Nd moment. Accordingly, no XMCD signal is measurable at low field.

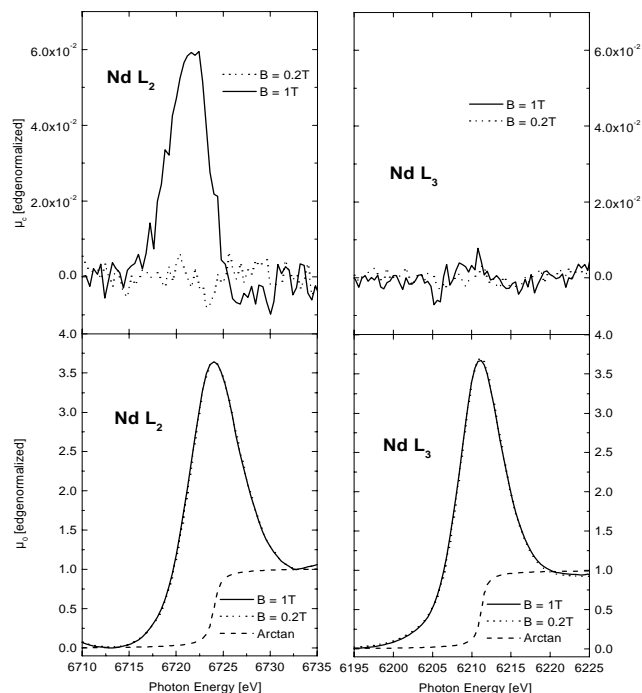


Figure 4
Nd L_2 , L_3 , μ_C and μ_0 normalized to the edge step

4. Conclusions

In $\text{La}_{1.2}\text{Nd}_{0.2}\text{Sr}_{1.6}\text{Mn}_2\text{O}_7$ the lanthanum $5d$ band is significant spin polarized. Also a weak XMCD signal is observed at the manganese K edge, which originates in a small polarization of the Mn $4p$ band. The pre-edge structures are dipole forbidden $1s \rightarrow 3d$ transitions, showing a small XMCD signal like $\text{La}_{0.7}\text{Ca}_{0.3}\text{MnO}_3$. As shown, the dichroic signals at the La L_2 , L_3 and Mn K edges follow the applied magnetic fields. A dominant orbital contribution is proved for the Nd $5d$ band. The Nd L_2 , L_3 XMCD signals could be interpreted by a strong $5d$ electron polarization. This may be explained with intra-atomic final state Coulomb interactions between the $2p \rightarrow 5d$ excited photoelectron and the

magnetically aligned $4f$ shell (Goedkoop 1997). The vanishing of Nd XMCD signals at 0.2T originates in the lattice hard-magnetically coupled Nd, due to its large orbital moment. This emphasizes the crucial role of the Nd for the metamagnetic transition in the system $\text{La}_{1.2}\text{Nd}_{0.2}\text{Sr}_{1.6}\text{Mn}_2\text{O}_7$ and has to be taken into account for further discussion.

We would like to thank the HASYLAB beamline A1 staff K. Attenkofer for support and help. This project is funded by the BMBF.

References

- Battle, P. D.; N. Kasimir, J. E. Millburn, M. J. Rosseinsky, R. T. Patel, L. E. Spring, J. F. Vente, S. J. Blundell, W. Hayes, A. K. Klehe, A. Mihut and J. Singleton (1998). *J. Appl. Phys.* **83**, 6379-6384.
- Baudelet, F.; J. P. Schillé, P. Saincavit, C. Brouder, C. Giorgetti, E. Dartyge and J. P. Kappler (1993). *J. El. Spec.* **62**, 153-166.
- Belli, M.; A. Scafati, A. Bianconi, S. Mobilio, L. Palladino, A. Reale and E. Burattini (1980). *Solid State Commun.* **35**, 355-361.
- Carra, P.; B. T. Thole, M. Altarelli and X. Wang (1993). *Phys. Rev. Lett.* **70**, 694-697.
- Chahara, K.; T. Ohno, M. Kasai, Y. Kanke and Y. Kozono (1993). *Appl. Phys. Lett.* **62**, 780-782.
- Dörr, K.; K.-H. Müller, K. Ruck, G. Krabbes and L. Schultz (1999). *J. Appl. Phys.* **85**, 5420-5422.
- Dörr, K.; K.-H. Müller, L. Schultz, K. Ruck and G. Krabbes (2000). *J. Appl. Phys.* **87**, 814-816.
- Galéra, R. M.; S. Pizzini, J. A. Blanco, J. P. Rueff, A. Fontaine, Ch. Giorgietti, F. Baudelet, E. Dartyge and M. F. López (1995). *Phys. Rev. B* **51**, 15957-15963.
- García, J.; J. Blasco, M. G. Proietti and M. Benfatto (1995). *Phys. Rev. B* **52**, 15823-15828.
- Goedkoop, J. B.; A. Rogalev, M. Rogaleva, C. Neumann, J. Goulon, M. Van Veenendaal and B. T. Thole (1997). *J. Phys. IV France* **7**, C2-415-420.
- Helmolt, R. von; J. Wecker, B. Holzapfel, L. Schultz and K. Samwer (1993). *Phys. Rev. Lett.* **71**, 2331-2333.
- Jo, T.; and S. Imada (1993). *J. Phys. Jpn.* **62**, 3721-3727.
- Kapusta, C.; R. Mycielski et al. (1996). *HASYLAB Annual Report I*, 321-322.
- Mahesh, R.; R. Mahendiran, A. K. Raychaudhuri and C. N. R. Rao (1996). *Solid State Chem.* **122**, 448-450.
- Miguel-Soriano, J.; J. Chaboy, L. M. García, F. Bartolomé and H. Maruyama (2000). *J. Appl. Phys.* **87**, 5884-5886.
- Millis, A. J.; P. B. Littlewood, B. I. Shraiman (1995). *Phys. Rev.* **74**, 5144-5147.
- Millis, A. J. (1998). *Phil. Trans. R. Soc. Lond.* **A356**, 1473-1480.
- Mitchell, J. F.; J. E. Millburn, M. Medarde, Dimitri N. Argyriou and J. D. Jorgensen (1999). *J. Appl. Phys.* **85**, 4352-4354.
- Moritomo, Y.; A. Asamitsu, H. Kuwahara and Y. Tokura (1996). *Nature* **380**, 141-144.
- Perring, T. G.; G. Aeppli, Y. Moritomo and Y. Tokura (1997). *Phys. Rev. Lett.* **78**, 3197-3200.
- Perring, T. G.; G. Aeppli, T. Kimura, Y. Tokura and M. A. Adams (1998). *Phys. Rev. B* **58**, R14693-R14696.
- Ruddlesden, S. N. and P. Popper (1958). *Acta Crystallogr.* **11**, 54-55.
- Seshardi, R.; A. Maignan, M. Hervieu, N. Nguyen and B. Raveau (1997). *Solid State Commun.* **101**, 453-457.
- Schütz, G. and D. Ahlers (1997). *J. Phys. IV France* **7**, C2-59-66.
- Subías, G.; J. García, M. G. Proietti and J. Blasco (1997). *Phys. Rev. B* **56**, 8183-8191.
- Thole, B. T., P. Carra, F. Sette and G. van der Laan (1992). *Phys. Rev. Lett.* **68**, 1943-1946.
- Wang, X.; T. C. Leung, B. N. Harmon and P. Carra (1993). *Phys. Rev. B* **47**, 9087-9090.
- Zener, C. (1951). *Phys. Rev.* **82**, 403-405.
- Zhao, G. -M.; K. Conder, H. Keller and K. A. Müller (1996). *Nature* **381**, 676-678.